LAWRENCE
LIVERMORE
NATIONAL
LABORATORY

LLNL-PROC-855783

Optical Damage Considerations in the Design of the Matter in ExtremeCondition Upgrade (MEC-U) Laser Systems

S. T. Yang, M. R. Greenberg, E. Cunningham, M. D. Martinez, R. A. Negres, T. M. Spinka, D. Alessi, S. Demos, A. Rigatti

October 10, 2023

SPIE Laser Damage
Dublin, CA, United States
September 17, 2023 through September 20, 2023

Disclaimer

Optical damage considerations in the design of the Matter in Extreme Condition Upgrade (MEC-U) laser systems

Steven T. Yang, Michael R. Greenberg, Eric Cunningham and Mikael D. Martinez

SLAC National Accelerator Laboratory, 2575 Sand Hill Road, Menlo Park, CA 94025 USA

Raluca A. Negres, Thomas M. Spinka and David Alessi

Lawrence Livermore National Laboratory, 7000 East Ave., Livermore CA 94550 USA

Stavros Demos and Amy Rigatti

Laboratory for Laser Energetics, University of Rochester, 250 East River Road, Rochester NY 14623-1299

Abstract

The Matter in Extreme Conditions Upgrade (MEC-U) project is a major upgrade to the MEC instrument of the LINAC Coherent Light Source (LCLS) X-ray free electron laser (XFEL) user facility at SLAC National Accelerator Laboratory. The envisioned MEC upgrade will significantly enhance the capabilities of the pump laser sources in current MEC experimental station, boosting the energy of the nanosecond shock driver from 100 J to the kJ level, and increasing the power and repetition rate of the short pulse laser from 25 TW at 5 Hz to 1 PW at 10 Hz rate. Building such high energy/power pump laser systems presents challenges to minimize and mitigate against laser-induced optical damage. As part of the system design, we have identified the optics at high-risk to damage and we have designed the laser systems to mitigate against these damage risks to ensure sustained facility operation.

1. Introduction

The Matter in Extreme Conditions Upgrade (MEC-U) project is a major upgrade to the MEC instrument of the LINAC Coherent Light Source (LCLS) X-ray free electron laser (XFEL) user facility at SLAC National Accelerator Laboratory [1,2]. As envisioned, a new cavern space, known as the eXtreme Experimental Hall (XEH), will be constructed at the end of the accelerator beamline as shown in Figs. 1(a)-(b). When completed, the XEH cavern will house a 4.5-meter diameter target chamber, together with two state-of-the-art laser systems: a kJ nanosecond long-pulse laser and a PW 10 Hz short pulse laser. By combining the bright x-ray source of the XFEL with world class high energy/power lasers, the MEC-U project will enable next generation experiments in high energy density physics and extreme matter science.

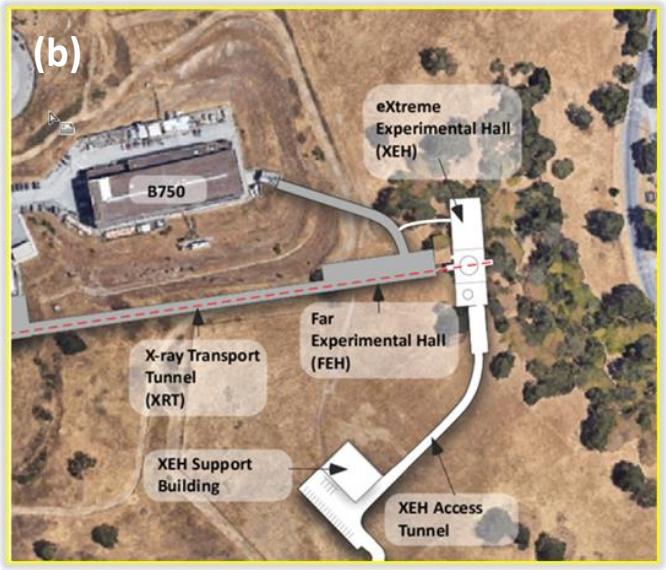

Fig. 1. Location of MEC-U facility. a) Overhead view of LCLS accelerator beamline, and b) close-up view of eXtreme Experimental Hall (XEH) located at the end of the accelerator beamline.

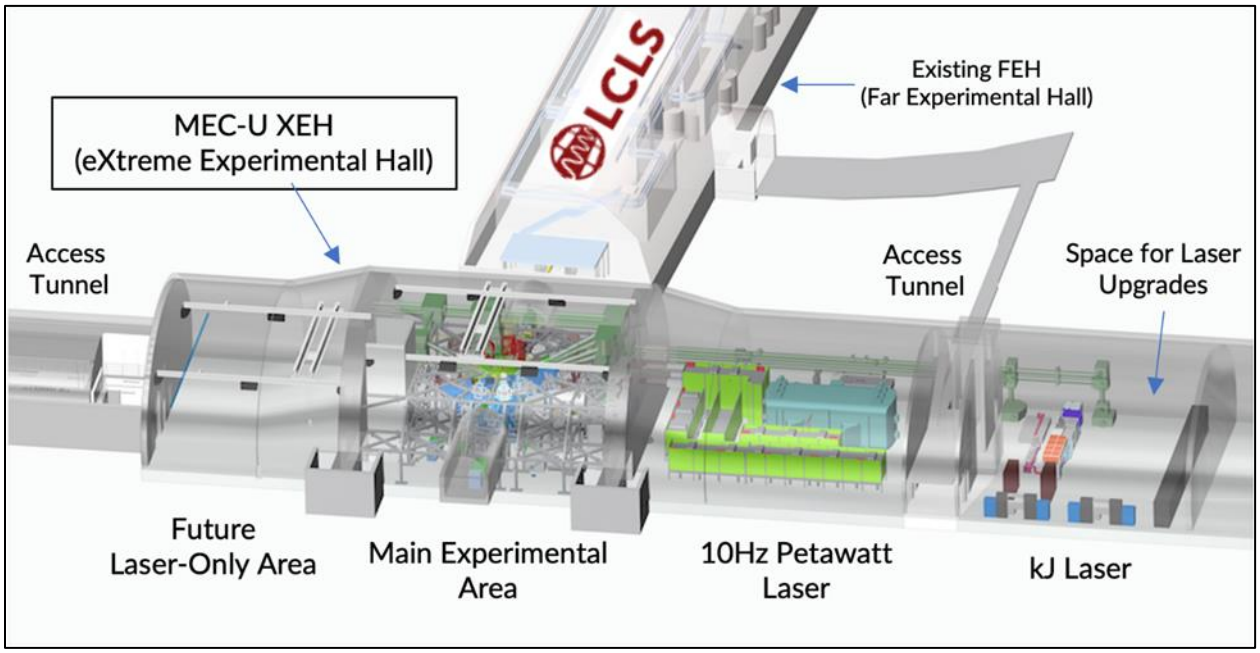

Fig. 2. Proposed XEH cavern layout with separate space for the target chamber and the two laser systems

The scale of the upgrade can be seen from the cavern layout in Fig. 2. The two laser systems will be housed in separate rooms in the cavern, and both are separated from the main experimental area containing the target chamber by a radiation shield wall. The kJ nanosecond long-pulse laser, hereafter refer to as the High-Energy Long-Pulse (HE-LP) laser, will be built by University of Rochester Laboratory of Laser Energetics (LLE). HE-LP laser architecture is based

on the Active Multi-pass Imaging Cavity Amplifier (AMICA) technology that has been developed at LLE. AMICA is essentially a miniaturized version of a multi-pass amplifier used in fusion class laser systems such as NIF and Omega EP. Within a compact footprint of 32'X6', AMICA module contains a Cavity Spatial Filter (CSF) for multi-passing the beam, a Pockels cell for switching the pulse in and out of the multi-pass amplifier, a deformable mirror for correcting prompt-induced wavefront distortion, and a 20-cm disk amplifier for amplification. The MEC-U HE-LP laser will use a AMICA module to amplify a seed source with pulse shaping capability. The output from the AMICA will be further amplified using an additional 20-cm disk amplifier booster to bring the 1ω energy up to the kJ range, before it is converted to harmonics at 2ω. The laser output requirement calls for 1kJ pulse energy at 2ω, with a shapeable pulse that can vary in duration from 0.5 to 30 ns, and a shot rate of 2 shots per hour. The baseline design is for one 2ω beamline. Potential future upgrade includes 1.25 kJ of 3ω energy each from up to four beamlines.

The PW 10 Hz short pulse laser, hereafter refer to as the Rep-Rated Short-Pulse (RR-SP) laser, will be built by Lawrence Livermore National Laboratory (LLNL) [3]. RR-SP is based on a Chirped Pulse Amplified (CPA) architecture with an Optical Parametric Chirped Pulse Amplification (OPCPA) front-end, and a diode-pumped, helium cooled, Nd:AGP1 laser slab power amplifier. The output from the power amplifier is compressed in a four grating compressor using meter-sized gratings. The underlying technologies for RR-SP laser have been previously demonstrated on the High-repetition-rate Advanced Petawatt Laser System (HAPLS) now in operation as the L3 laser at ELI beamline [4]. The short pulse laser output requirement calls for output pulse energy up to 164 Joule, with a pulse duration that is adjustable from transform-limited pulse width of 150 fs to 10 ps chirped pulse, a repetition rate of 10 Hz, and a peak power of 1 PW with a focal intensity at target of at least 10^{21} W/cm^2. Potential future upgrade includes the possibility of adding a second RR-SP laser.

To deliver the laser output to the target chamber, separate beam transport systems for the two laser systems will be designed and built. Each beam transport spans the ~50-meter length of the cavern from laser room to the target area. To minimize beam modulation due to diffractive propagation, the laser output will be image-relayed to the final optics at the target chamber using refractive and a reflective relay-telescopes in HE-LP and RR-SP beam transports. Because of the high energy and intensity of the lasers, beam sizes on beam transport optics are in the tens of centimeter to half a meter size. Owing to the high power of RR-SP beam, the entire RR-SP beam transport will be in vacuum. The HE-LP beam transport will be enclosed but in air, except for the region inside the vacuum relay telescope. The final optics section contains optics for focusing the beam to desired focal spot size at target and for pointing to target.

Designing and building such a high energy and power laser systems plus beam transports present many technical challenges. Top among them is the risk of optics damage. In our design, optics with high damage risk include 1) HE-LP and RR-SP beam transport optics, 2) RR-SP laser compressor diffraction grating, and 3) RR-SP final focusing optics. For each of these high-risk optics, we will describe in the following sections how we assessed the damage threat, and how we have designed the laser system to minimize optics damage to these optics to ensure sustained long-term operation of the facility.

2. Damage threat to beam transport optics: High Energy Long Pulse

For transporting the HE-LP laser from the laser to target chamber, harmonically coated green (2ω) or UV (3ω) High Reflector (HR) mirrors will be needed. To assess the damage threshold of 2ω and 3ω HR mirrors, we leveraged data from thin film damage competitions organized as part of the SPIE Laser damage symposia in recent years. For instance, 2020 damage competition surveyed 532 nm HR coating LIDT at normal incidence using raster scan test, which scans a small test beam over an area of approximately 1 cm^2 [5]. The result showed that 12 out of 30 total samples submitted had a threshold of at least 20 J/cm^2 for damage initiation of stable defects. In 2017, damage competition examined 355 nm HR mirror coating with 45^o Angle-Of-Incidence (AOI) and P-polarization [6]. From that study, using raster scan test, coating samples from participating vendors showed damage threshold ranging from 1 J/cm^2 to 14 J/cm^2, with 6 out of 35 submitted samples having LIDT of at least 10 J/cm^2. These data from the damage competitions gave us an estimate of practically achievable coating damage thresholds. Starting with these estimated damage threshold values, we then

applied adjustments to arrive at maximum safe operating fluence for our operating point. For 2ω HR case, we assume 20 J/cm^2 coating LIDT is achievable with 6-ns pulse irradiation from the survey data. We then apply a square root temporal scaling between our use pulse duration (3.1 ns) versus the test pulse (6 ns) to the damage threshold. Next, we derate the threshold by a factor of two to extrapolate from small beam test used in raster scan measurement to large beam LIDT. Raster scan test is supposed to yield LIDT for large beam by scanning over a larger area to sample the low-density pre-cursors with lower damage threshold. However, the use of raster scan data to approximate large beam LIDT remains uncertain. To be conservative, we elected to derate the raster scan threshold by a factor of two to account for the large beam effect. Finally, we drop the damage threshold by a factor of two to allow for as much as 2:1 peak-to-mean beam fluence modulation to arrive at a maximum safe operating mean fluence of 3.6 J/cm^2 for 2ω HR coating. Following similar analysis and starting with damage threshold of 10 J/cm^2 for 3ω HR coating at 5-ns pulse irradiation, we estimate a maximum safe operating mean fluence value of 3.1 J/cm^2 at 3ω.

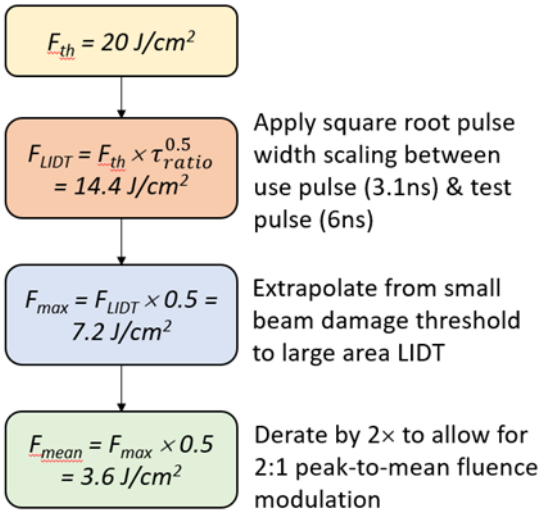

Fig. 3. Steps for deriving maximum safe operating fluence starting with published damage threshold data for 2ω HR coating.

Once the maximum operating fluence limit has been determined, we can then choose the beam size to ensure that the beam fluence on any beam transport optics remain below the maximum permissible level. For HE-LP beam, the beam profile can be modeled as a circular top-hat beam with 10th order super-Gaussian profile. To provide some margin against damage, we chose a beam diameter of 19 cm and 28 cm (at 1% fluence level relative to peak), for 2ω and 3ω beams respectively. Assuming 1 kJ and 1.25 kJ laser output at 2ω and 3ω, the chosen beam size yielded mean fluence that gave safety factors of 1.2× and 1.7× respectively relative to maximum safe operating mean fluence.

3. Beam Transport Optics: Rep Rated Short Pulse

For transporting RR-SP laser from output to target chamber, 1-μm Multi-Layer Dielectric (MLD) HR coated mirrors will be needed. For estimating the damage threshold of 1-μm MLD mirrors, we start with the damage threshold of a single layer from the MLD stack and equating it to the damage threshold of the MLD coating containing such a layer [7]. For Ta_2O_5 thin film used in typical near-IR MLD coating, a damage threshold of 1.1 J/cm^2 when tested with 1030 nm 500 fs laser pulse has been reported [8]. The choice of Ta_2O_5 as our starting point is conservative since it has lower damage threshold due to its lower bandgap as compared to the more typically used HfO_2 material. Scaling to 150 fs for our use case yields a damage threshold of 0.77 J/cm^2 using a pulse width scaling exponent of 0.3 [9]. This single layer intrinsic damage threshold is then derated by 1/3 to 0.5 J/cm^2 to account for multi-pulse cumulative damage threshold, which is attributed to “incubation” effect that arises from accumulation of laser-induced traps with energy lower than the bandgap [10]. The 0.5 J/cm^2 damage threshold arrived at after applying the “incubation” adjustment is comparable to reported

damage growth threshold from nodule defects in MLD coatings [11]. Additional threshold reduction of 20% is applied for use in vacuum environment [12]. Finally, a factor of two reduction is taken to allow for up to 2:1 peak to mean fluence modulation, resulting in a maximum safe operating mean fluence limit of 0.2 J/cm^2 for 1-µm HR MLD coating. Assuming 164 J at the laser output and with a rectangular beam footprint with 10th order super-gaussian profile, the maximum mean fluence on the transport optics is 0.15 J/cm^2, providing a safety factor of 1.33× relative to maximum safe operating limit.

Real beam has finite spatial modulations due to gain non-uniformity, phase to amplitude conversion from wavefront aberrations and particle contaminations on optics [13]. To ensure that the maximum beam fluence does not exceed the damage threshold, it is necessary that the mean fluence remains below 0.2 J/cm^2 *AND* the peak-to-mean modulation is less than 2:1 on all transport optics. To verify that these conditions are met for our design, physical optics propagation simulations were carried out using representative HAPLS beam profile as input and assuming optics wavefront from existing similar optics or vendor specifications. The result of the propagation simulation shows that mean fluence and peak-to-mean modulation both reach a maximum at the first Off-Axis-Parabolic (OAP) mirror of the reflective relay telescope with values of 0.15 J/cm^2 and 1.66:1, confirming that beam fluence on all transport optics are below damage threshold with margin.

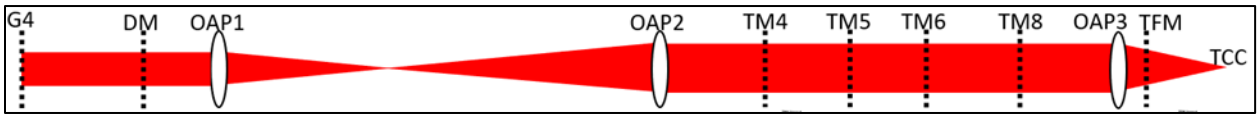

a)

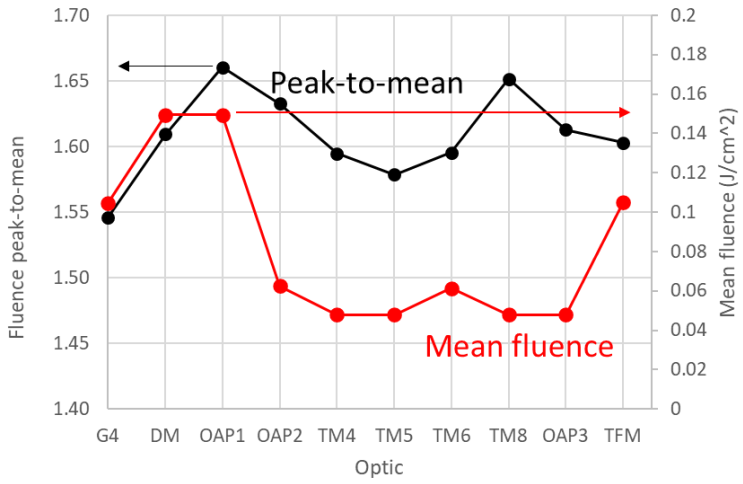

b)

Fig. 4. Physical optics propagation simulation of RR-SP beam transport. (a) unfolded RR-SP beam transport path. lens depicted is mean to represent reflective mirrors, and (b) calculated mean fluence and peak-to-mean modulation on beam transport optics.

So far, the analysis and design are based on published damage threshold values from vendor survey. To certify that the assumed coating damage threshold can be met, we intend to conduct qualification test of coating witness samples from vendors. For these qualification tests, we will be relying on commercial optics damage service facilities. As a test protocol, we plan to use a raster scan test to survey density of low damage threshold precursors over at least 1 cm^2 area. This is to be followed by damage growth test on sites that have initiated during raster scan. Since damages that initiate but does not grow during subsequent shots do not materially impact the optics lifetime, it is important to know both the

damage initiation and growth thresholds, especially for low repetition rate system such as the HE-LP laser. Ideally, we would like to perform damage test under realistic use conditions of large beam footprint and high repetition rate. For this purpose, we are interested in engaging with facilities such as LLNL's Optical Science Laser (OSL) with up to 13 cm size beam, and with HILASE's Bivoj laser with its 10mmX10mm beam footprint and 10 Hz repetition rate for optics damage testing [14,15].

4. Diffraction Grating

For RR-SP laser, the chirped pulse amplified architecture calls for the use of meter-size MLD diffraction gratings in the final compressor stage to compress the stretched pulse to hundreds of fs pulse duration. A survey of operating fluence and grating damage threshold from similar short pulse laser facilities have been compiled by D. Alessi from LLNL and it is shown in Fig. 5 [16]. Compare with similar facilities, such as the Texas PW and ELI L4 beamlines which operate at fluence of 0.7 J/cm^2 and 0.4 J/cm^2 respectively, the fluence on the MEC-U final grating is at least 2× lower.

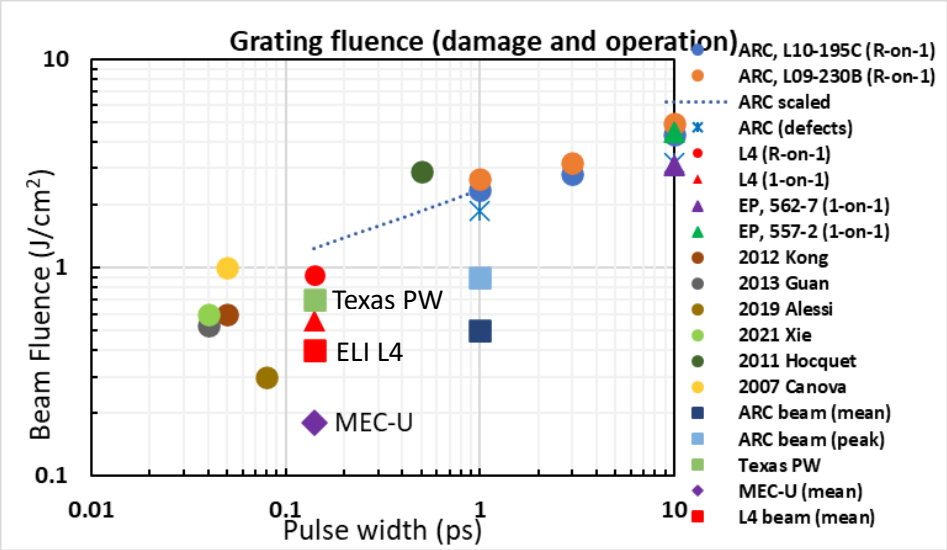

Fig. 5. Survey of operating fluence / damage threshold of MLD diffraction gratings from short pulse laser facilities as compiled by D. Alessi of LLNL [13].

To further reduce damage risk to the expensive meter-scale MLD grating, LLNL team plans to introduce spatial chirp at the compressor output to smooth the beam profile and reduce beam spatial modulation peak-to-mean. Similar schemes have been proposed and implemented previously [17,18]. One approach for inducing spatial chirp is to introduce mismatch in the slant distance between the two grating pairs in a four grating compressor setup, such as is shown in Fig. 6. The mismatch in slant distance between the two grating pairs results in spatial displacement of the different spectral components of the beam on the final grating. The spatial dispersion is defined as the increase in the width D of the output beam relative to the input. To assess the amount of dispersion required to achieve the desired beam smoothing, beam modulation peak-to-mean as a function of spatial chirp has been calculated assuming Gaussian shaped hot spots with different FWHM widths, ranging from 1 mm to 6 mm [18]. In all cases, the beam modulation peak-to-mean drops as amount of spatial dispersion D is increased, with the modulation of the smallest Gaussian hot spot dropping the fastest. In addition to the ideal Gaussian shaped hot spot, we also examined the peak-to-mean of beam modulation assuming a realistic beam profile taken from HAPLS laser. The modulation decrease follows similar trend. From these calculations, we find a spatial dispersion amount of 20 mm is a good compromise in reducing beam modulation while not significantly increasing the spatially dispersed output beam size.

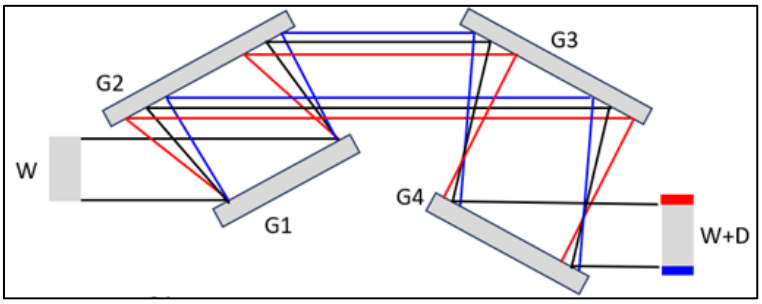

Fig. 6. 4-grating compressor configuration with mismatch in the slant distance between the two pairs of gratings to introduce spatial dispersion at output grating G4.

One concern about introducing spatial chirp at compressor output is whether it would have any impact on beam intensity at and near focus. To assess impact of residual spatial chirp on focal intensity, spatiotemporal calculations with a spatially chirped beam has been carried out. Fig. 7 shows the calculated spatial-time intensity profile I(x,t) at focus and at 10 mm before focus, for the case without and with D=20 mm spatial chirp. The calculation assumed a super-Gaussian spatial profile and 150 fs FWHM pulse duration. As expected, with no spatial chirp, the focal spot is diffraction limited, while the temporal profile is transform-limited at 150 fs. With residual spatial chirp of 20 mm, the spatiotemporal profile shows a slight tilt, indicative of Pulse-Front Tilt (PFT). The PFT is small, however, such that the spatial profile at pulse peak I(x,t=0) and the temporal profile at target center I(x=0,t) are identical between the no chirped and chirped cases. At focus offset of -10 mm, the spatiotemporal profiles are nearly the same between the two cases, except for a slight distortion at the edge of the beam. Comparing the intensity and temporal lineout at t=0 and x=0, the two cases are identical. These calculations confirm that the proposed residual spatial chirp does not impact peak intensity at and near focus.

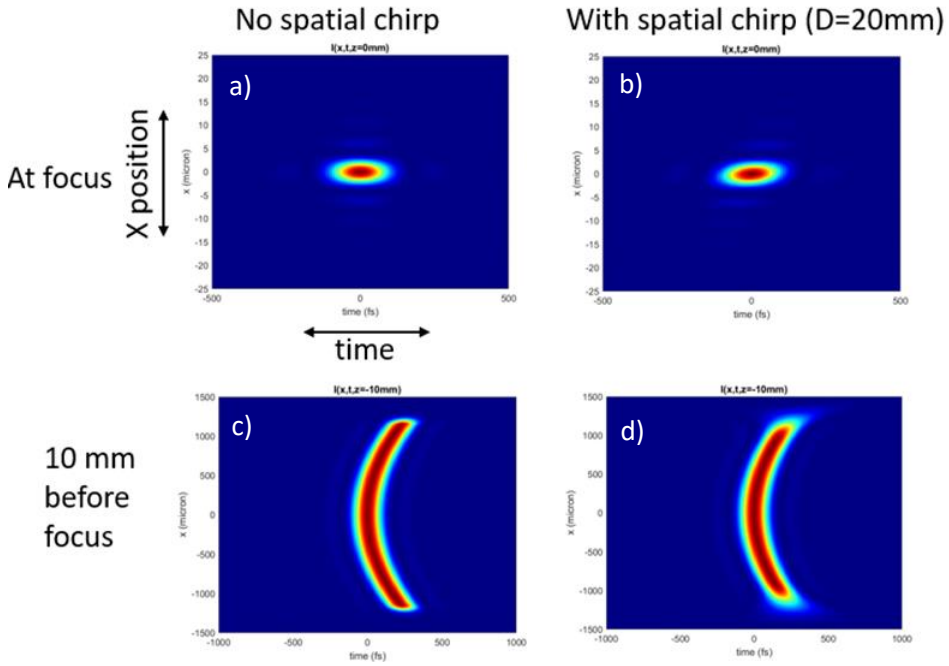

Fig 7. Calculated spatiotemporal profile I(x,t) for the case of a) no spatial chirp (D=0mm) and at focus (z=0mm), b) with D=20mm and z=0mm, c) D=0mm and at 10 mm before focus (z=-10mm), and d) D=20mm and z=-10mm

5. Final Focusing Optics

Target debris from experiments using the high energy and power lasers can contaminate the final focusing optics and compromise their optical performance. Traditionally, final optics has been shielded from target debris using debris shield made of thin glass plate. This is the strategy that we will use for protecting vacuum window and final focusing lens in the HE-LP beamline. For RR-SP laser, use of debris shield is impractical due to B-integral limitations which introduce unacceptable distortion to the pulse. To protect the expensive final focusing OAP from target debris and shrapnel, we added a flat turning mirror, known as the Target Facing Mirror (TFM), after the OAP, to shield OAP from direct line-of-sight to the target. The flat turning mirror, located 1.35 m away from the target, is expected to degrade due to target debris contamination. As part of the concept of operation, we plan to monitor the reflectance of the TFM in-situ using a reflective target that sends the alignment beam back to the source. The TFM will be replaced when its reflectance drops below a set threshold. For reference, the Omega EP final focusing OAP, positioned 1 meter away from the target, is exchanged after ~400-450 shots, when its reflectance drops by more than 20% [19]. Given the Omega-EP short pulse laser shot rate of ~10-20 shots per week, the exchange occurs at a frequency of every 6-months to a year. Extrapolating to the case of RR-SP laser operating at 10 Hz, 400 shots lifetime implies TFM exchanges on a daily or weekly basis, with significant operational cost implications. Therefore, mitigating target debris induced optics degradation for high repetition rate laser remains a challenge.

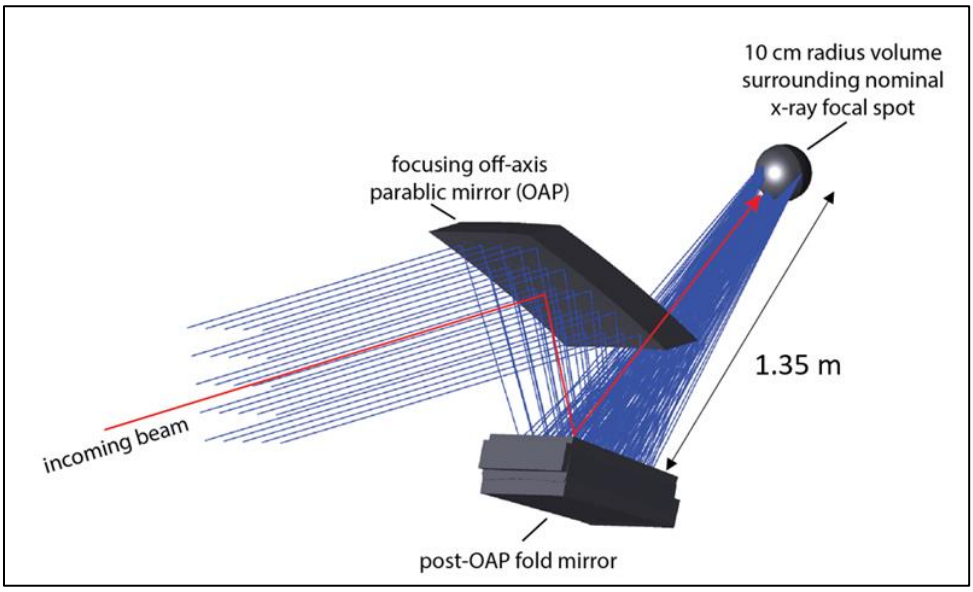

Fig. 8. RR-SP final focusing geometry where a flat folding mirror is located after the final focusing OAP to shield the OAP from direct line of sight to target. Distance of flat folding mirror to target is 1.35 meter.

6. Conclusion

Optics damage threat is a primary technical challenge in the planned MEC-U project. Optics with high damage risk include the beam transport optic, the compressor gratings, and the final focusing optics. For these high-risk optics, we have assessed the damage threshold based on published data and expert advice. Scaling from threshold data to the MEC-U use condition, we have determined the safe operating limit. To ensure that we minimize damage, the beam size on critical optics have been chosen to yield mean fluence that is below maximum safe operating limit with margin. To further reduce fluence on gratings, we are proposing to intentionally introduce spatial chirp to smooth out beam fluence on the final grating. During the design and build phase of the project, we plan to damage test coating samples to qualify

the vendor and to ensure that as-delivered coating meets our expectations. Mitigating damage threat to final focusing optics due to target debris remains a challenge, especially for MEC-U's high repetition rate short pulse laser system.

Acknowledgement

The MEC-U project is supported by the U.S. Department of Energy, Office of Science, Office of Fusion Energy Sciences under Contract No. DE-AC02-76SF00515. Portions of this work were performed in part under the auspices of the U.S. Department of Energy by Lawrence Livermore National Laboratory under Contract DE-AC52-07NA27344, with funding provided by the DOE Office of Fusion Energy Sciences and in part supported by the Department of Energy National Nuclear Security Administration under Award Number DE-NA0003856, the University of Rochester, and the New York State Energy Research and Development Authority.

References

[1] F. Batysta, J. Bauer, K. Belt, D. Bhogadi, A. Conder, E. Copitch, E. Cunningham, C. B. Curry, A. M. Dunne, G. Dyer, M. Edwards, I. Evans, B. Fishler, F. Fiuza, L. Fletcher, A. Fry, J. Galbraith, E. Galtier, T. Galvin, M. Gauthier, A. Gleason, S. Glenzer, S. Green, M. Greenberg, C. Hardin, P. Hart, P. Heimann, E. Hill, T. Johnson, H. J. Lee, K. LeFortune, T. Liang, M. Martinez, E. McBride, M. Mo, E. Moses, B. Nagler, B. Ofori-Okai, B. Reagan, S. Reyes, C. Rossignol, R. Sandberg, C. Schoenwaelder, J. Sims, E. Sistrunk, T. Spinka, V. Tang, J. Thayer, F. Treffert, A. Wallace, W. White, S. Wilks, J. Yin, and J. Zuegel. Matter in Extreme Conditions Upgrade conceptual design report. Technical Report SLAC-R-1152, SLAC National Accelerator Laboratory, 2021.

[2] G. Dyer, E. Galtier, E. Cunningham, C.B. Curry, L. Fletcher, F. Fiuza, S. Glenzer, A. Gleason, B. Nagler, H.J. Lee, D. Khaghani, M. Gauthier, A. Conder, M. Martinez, K. LaFortune, C. Hardine, B. Arnold, S. Yang, M. Greenberg, T. Spinka, V. Tang, E. Hill, J.D. Zuegel, S.Z. Green, and A. Fry, "The MEC-U Project at LCLS," CLEO paper JTh2A.72 (2023).

[3] B.A. Reagan, M. Albrecht, D. Alessi, M. Ammons, S. Banerjee, C. Barillas, F. Batysta, B. Buckley, A. Chemali, E. Clark, E. Davila, R.J. Deri, K. Eseltine, B. Fishler, E.S. Fukerson, J. Galbraith, T. Galvin, A. Gonzales, V. Gopalan, S. Herriot, Z. Hubka, J. Jimenez, L. Kiani, E. Koh, R. Kupfer, Z. Liao, J. Lusk, H. Nguyen, A. Patel, A. Peer, J. Peterson, R. Plummer, K. Schaffers, E. Sistrunk, T.M. Spinka, C. Stolz, I. Tamer, V. Tang, S. Telford, K. Terzi, P. Utley, K.M. Velas, A. Vella, J.N. Wong, "High repetition rate, high energy petawatt laser for the matter in extreme conditions upgrade," Proc. SPIE 12401, High Power Lasers for Fusion Research VII, 124010A (2023).

[4] E. Sistrunk, T. Spinka, A. Bayramian, S. Betts, R. Bopp, S. Buck, K. Charron, J. Cupal, R. Deri, M. Drouin, A. Erlandson, E. S. Fulkerson, J. Horner, J. Horacek, J. Jarboe, K. Kasl, D. Kim, E. Koh, L. Koubikova, R. Lanning, W. Maranville, C. Marshall, D. Mason, J. Menapace, P. Miller, P. Mazurek, A. Naylon, J. Novak, D. Peceli, P. Rosso, K. Schaffers, D. Smith, J. Stanley, R. Steele, S. Telford, J. Thoma, D. VanBlarcom, J. Weiss, P. Wegner, B. Rus, and C. Haefner, "All Diode-Pumped, High-repetition-rate Advanced Petawatt Laser System (HAPLS)," in Conference on Lasers and Electro-Optics, OSA Technical Digest (online) (Optica Publishing Group, 2017), paper STh1L.2.

[5] R.A. Negres, C.J. Stolz, G. Batavičiūtė, and A. Melninkaitis, "532-nm, nanosecond laser mirror thin film damage competition," Proc. SPIE 11514, 115140L (2020).doi: 10.1117/12.2566691

[6] R.A. Negres, C.J. Stolz, M.D. Thomas, M. Caputo, "355-nm, nanosecond laser mirror thin film damage competition," Proc. SPIE 10447, 104470X (2017).doi: 10.1117/12.2279981

[7] A. Hervy, L. Gallais, G. Chériaux, D. Mouricaud, "Femtosecond laser-induced damage threshold of electron beam deposited dielectrics for 1-m class optics," Opt. Eng. 56(1), 011001 (2016).doi: 10.1117/1.OE.56.1.011001

[8] L. Gallais and M. Commandré, "Laser-induced damage thresholds of bulk and coating optical materials at 1030 nm, 500 fs," Appl. Opt. 53, A187 (2014). http://dx.doi.org/10.1364/AO.53.00A186

[9] J. Mero, J. Liu, and W. Rudolph, D. Ristau and K. Starke, “Scaling laws of femtosecond laser pulse induced breakdown in oxide films,” Phys. Rev. B 71, 115109 (2005). Doi: 10.1103/PhysRevB.71.115109

[10] M. Mero, B. Clapp, J.C. Jasapara, W. Rudolph, D. Ristau, K. Starke, J. Krüger, S. Martin, and W. Kautek, “On the damage behavior of dielectric films when illuminated with multiple femtosecond laser pulses,” Opt. Eng. 44(5), 051107 (2005). https://doi.org/10.1117/1.1905343

[11] L. Gallais, X. Cheng, and Z. Wang, “Influence of nodular defects on the laser damage resistance of optical coatings in the femtosecond regime,” Opt. Lett. 39, 1545-1548 (2014). http://dx.doi.org/10.1364/OL.39.001545

[12] K.R.P. Kafka, N. Talisa, G. Tempea, D.R. Austin, C. Neacsu, and E.A. Chowdhury, “Few-cycle pulse laser induced damage threshold determination of ultra-broadband optics,” Opt. Exp. 24, 28858-28868 (2016). http://dx.doi.org/10.1364/OE.24.028858

[13] K. R. P. Kafka and S. G. Demos, “interaction of short laser pulses with model contamination microparticles on a high reflector”, Opt. Lett. **44**, 1844-1847 (2019). https://doi.org/10.1364/OL.44.001844

[14] M. C. Nostrand, T. L. Weiland, R. L. Luthi, J. L. Vickers, W. D. Sell, J. A. Stanley, J. Honig, J. Auerbach, R. P. Hackel, and P. J. Wegner, “A large-aperture high energy laser system for optics and optical component testing,” Proc. SPIE 5273, 325–333 (2004). doi: 10.1117/12.528327

[15] M. Divoký, J. Pilař, M. Hanuš, P. Navrátil, O. Denk, P. Severová, P. Mason, T. Butcher, S. Banerjee, M. D. Vido, C. Edwards, J. Collier, M. Smarž, and T. Mocek, “150 J DPSSL operating at 1.5 kW level,” Opt. Lett. 46, 5771-5773 (2021). https://doi.org/10.1364/OL.444902

[16] Data and plot supplied by D. Alessi of LLNL.

[17] N. Blanchot, E.B.G. Behar, C. Bellet, D. Bigourd, F. Boubault, C. Chappuis, H. Coïc, C. DAmiens-Dupont, O. Flour, O. Hartmann, L. Hilsz, E. Hugonnot, E. Lavastre, J. Luce, E. Mazataud, J. Neauport, S. Noailles, B. Remy, F. Sautarel, M. Sautet, and C. Rouyer, “Experimental demonstration of a synthetic aperture compression scheme for multi-Petawatt high-energy lasers,” Opt. Express, 18, 10088-10097 (2010). https://doi.org/10.1364/OE.18.010088

[18] X. Shen, S. Du, W Liang, P. Wang, J. Liu, R. Li, “Two-step pulse compressor based on asymmetric four-grating compressor for femtosecond petawatt lasers,” Appl. Phys. B 128, 159 (2022). https://doi.org/10.1007/s00340-022-07878-9

[19] private communication from University of Rochester, LLE.